



Original Article

Int Neurourol J 2022;26(Suppl 2):S94-105

<https://doi.org/10.5213/inj.2244252.126>

pISSN 2093-4777 · eISSN 2093-6931



Changes in the Neuronal Architecture of the Hippocampus in a 6-Hydroxydopamine-Lesioned Rat Model of Parkinson Disease

Bohye Kim¹, Poornima D. E. Weerasinghe-Mudiyanselage¹, Mary Jasmin Ang¹, Jeongmin Lee¹, Sohi Kang¹, Jong-Choon Kim¹, Sung-Ho Kim¹, Joong-Sun Kim¹, Chaeyong Jung², Taekyun Shin³, Changjong Moon¹

¹Department of Veterinary Anatomy and Animal Behavior, College of Veterinary Medicine and BK21 FOUR Program, Chonnam National University, Gwangju, Korea

²Department of Anatomy, Chonnam National University Medical School, Gwangju, Korea

³Department of Veterinary Anatomy, College of Veterinary Medicine, Jeju National University, Jeju, Korea

Purpose: Parkinson disease (PD) is a progressive neurodegenerative disorder in which dopaminergic (DAergic) systems are destroyed (particularly in the nigrostriatal system), causing both motor and nonmotor symptoms. Hippocampal neuroplasticity is altered in PD animal models, resulting in nonmotor dysfunctions. However, little is known about the precise mechanism underlying the hippocampal dysfunctions in PD.

Methods: Striatal 6-hydroxydopamine (6-OHDA) infusions were performed unilaterally in adult Sprague Dawley rats. Both motor and nonmotor symptoms alongside the expression of tyrosine hydroxylase (TH) in the *substantia nigra* and striatum were confirmed in 6-OHDA-lesioned rats. The neuronal architecture in the hippocampus was analyzed by Golgi staining.

Results: During the 7–8 weeks after infusion, the 6-OHDA-lesioned rats exhibited motor and nonmotor dysfunctions (especially anxiety/depression-like behaviors). Rats with unilateral 6-OHDA infusion displayed reduced TH+ immunoreactivity in the ipsilateral nigrostriatal pathway of the brain. Golgi staining revealed that striatal 6-OHDA infusion significantly decreased the dendritic complexity (i.e., number of crossing dendrites, total dendritic length, and branch points) in the ipsilateral hippocampal conus ammonis 1 (CA1) apical/basal and dentate gyrus (DG) subregions. Additionally, the dendritic spine density and morphology were significantly altered in the CA1 apical/basal and DG subregions following striatal 6-OHDA infusion. However, alteration of microglial and astrocytic distributions did not occur in the hippocampus following striatal 6-OHDA infusion.

Conclusions: The present study provides anatomical evidence that the structural plasticity in the hippocampus is altered in the late phase following striatal 6-OHDA infusion in rats, possibly as a result of the prolonged suppression of the DAergic system, and independent of neuroinflammation.

Keywords: 6-hydroxydopamine; Dopaminergic system; Golgi staining; Nonmotor symptom; Parkinson disease; Structural plasticity

- **Grant/Fund Support:** This work was supported by the National Research Foundation (NRF) of Korea grant funded by the Korean Government (NRF-2019R1A2C1004045; NRF-2022R1A2C1004022).
- **Research Ethics:** All the experimental and animal handling procedures were performed in accordance with the guidelines of the institutional care and use committee of Chonnam National University (22 April 2021; CNU IACUC-YB-2021-40), and animal care conformed to internationally agreed standards for laboratory animal use and care, as dictated by the National Institutes of Health (NIH).
- **Conflict of Interest:** No potential conflict of interest relevant to this article was reported.

Corresponding author: Changjong Moon

<https://orcid.org/0000-0003-2451-0374>

Department of Veterinary Anatomy, College of Veterinary Medicine and BK21 FOUR Program, Chonnam National University, 77 Yongbong-ro, Buk-gu, Gwangju 61186, Korea

Email: moonc@chonnam.ac.kr

Submitted: October 8, 2022 / **Accepted after revision:** November 15, 2022



This is an Open Access article distributed under the terms of the Creative Commons Attribution Non-Commercial License (<http://creativecommons.org/licenses/by-nc/4.0/>) which permits unrestricted non-commercial use, distribution, and reproduction in any medium, provided the original work is properly cited.

• HIGHLIGHTS

- Striatal 6-hydroxydopamine (6-OHDA) infusion induced behavioral dysfunctions and reduced DAergic signaling in rat brains.
- Structural plasticity is altered in the hippocampus of 6-OHDA-lesioned rats.
- Hippocampal dysfunctions may be related to the alteration of structural plasticity in Parkinson disease animal models, possibly by a decrease in DAergic signaling.

INTRODUCTION

Parkinson disease (PD) is the world's second most common neurodegenerative disorder [1]. It is distinguished by a significant loss of dopaminergic (DAergic) neurons, primarily in the *substantia nigra* (SN), and results in a decrease in DAergic fibers in the striatum [2]. Additionally, PD is a neurological disease that causes both motor and nonmotor symptoms [3]. The main clinical focus in PD has been on motor symptoms; nevertheless, there is growing acknowledgment that the clinical spectrum of PD is more comprehensive, and includes nonmotor functions [4]. The most prevalent nonmotor symptoms in PD are depression, anxiety, cognitive decline, pain, fatigue, insomnia, and autonomic dysfunction. Furthermore, approximately 40%–50% of PD patients are diagnosed with anxiety or depression [5]. Moreover, the nonmotor symptoms that are associated with the hippocampus significantly affect PD patients' quality of life [6].

Since DAergic damage is a defining characteristic of PD, the structural, molecular, and functional alterations in the nigrostriatal system have garnered much attention [7]. However, research on the other brain regions in PD is needed to clarify their roles, their interaction with the nigrostriatal system, and their involvement in the mechanism underlying nonmotor dysfunctions. The hippocampus is critical for cognitive and emotional regulation and receives DAergic projections from the ventral tegmental area and SN, respectively [8]. Dopamine (DA) modulates hippocampal long-term potentiation (LTP) [9]. In PD, the DAergic system interacts with the synaptic plasticity of the hippocampus [10], and the hippocampus is implicated in the nonmotor dysfunctions of PD [8]. In preclinical PD studies, synaptic mechanisms underlying hippocampal dysfunction were reported in neurotoxic and genetic animal models of PD, including 6-hydroxydopamine (6-OHDA)-lesioned rats [11] and α -synuclein transgenic mice [12], respectively.

Neuroplasticity refers to the capacity of neuronal networks in the brain that change through development and reorganization; it is typically classified as structural and functional plasticity [13,14]. Structural plasticity, such as dendritic formation and

spine development, is controlled by the regulation of the neuronal actin cytoskeleton [15]. Neurodegenerative diseases may be caused by dendritic and spine alterations produced by acute or chronic disruptions in brain tissue homeostasis [16]. Structural plasticity in the hippocampus can be influenced by a variety of stimuli, some of which appear to have long-term effects [8]. Previous studies found that dendritic complexity and/or spine density was altered in 1-methyl-4-phenyl-1,2,3,6-tetrahydropyridine (MPTP)-lesioned [17,18] and leucine-rich repeat kinase 2-mutant mouse PD models [19,20]. However, many questions remain unanswered about the functional and structural changes of hippocampal neurons that occur in PD. In this study, a hemiparkinsonian rat model with an ipsilaterally striatal infusion of 6-OHDA was used, which mimics features of the human pathological condition of PD [21]. Therefore, this study attempted to analyze behavioral impairments and alteration of structural plasticity in the hippocampus, as well as explain their correlations in this animal model.

MATERIALS AND METHODS**Animals and Surgical Procedure**

Male Sprague Dawley rats weighing 250–300 g were obtained from Charles River Laboratories (Wilmington, MA, USA) at 8 weeks old and allowed to acclimate for 1 week prior to use in the study. The rats were immobilized in a stereotaxic device (SR-6; NARISHIGE, Tokyo, Japan) with a flat head position after anesthesia. The coordinates were as follows: anteroposterior, +1.3, +0.4, -0.4, -1.3 mm from the bregma; mediolateral, -2.6, -3.0, -4.2, -4.5 mm from the midline; and dorsoventral, -5.0, respectively, from the skull. Per rat: the 6-OHDA (3.5 mg/mL, Sigma-Aldrich, St. Louis, MO, USA) was administered into the right striatum with an infusion pump using an 8 μ L saline with 0.02% (w/v) ascorbic acid (Wako, Osaka, Japan) through a 10.5- μ L microinjection cannula at a continuous flow rate of 1 μ L/min (2 μ L was injected at each coordinate). Sham-operated rats were subjected to the identical method, except instead of 6-OHDA, 8 μ L of the vehicle (0.9% saline containing 0.02% (w/v) ascorbic acid) was injected into the striatum.

Behavioral Analysis of Motor Symptoms

Apomorphine-induced rotation test

Four weeks after striatal 6-OHDA infusion, apomorphine hydrochloride (1 mg/kg; Wako) was given intraperitoneally into the rats. The number of left-handed (contralateral) rotations was monitored for 30 minutes. Hemiparkinsonian rat models for PD were found to have a rotational velocity of more than 7 turns/min.

Open field test

The equipment was made from an acrylic chamber (width [W] × depth [D] × height [H]: 60 × 60 × 30 cm). The rats were carefully placed in the center of the open field. Using Smart-Scan (Panlab, Barcelona, Spain), the proportion of entries and duration in the total movement time (s), total distance traveled (cm), and margin time (s) were calculated over 30 minutes.

Cylinder test

The test was performed as follows: individual rats were placed within a glass cylinder (diameter, 22 cm; height, 26 cm) with one mirror set below the cylinder at a 45° angle to provide 360° viewing. The rats were videotaped for 5 minutes following initial contact with the walls of the cylinder with their impaired, unimpaired, or both forelimbs. The scores were computed using the asymmetry ratio, left-right/(right + left + both). The forelimb asymmetry ratio scores vary from 1 to 1. The positive ratio indicates that the unimpaired forelimb is utilized more than the impaired forelimb. The negative asymmetry ratio shows that the impaired forelimb is used more than the unimpaired forelimb.

Behavioral Analysis of Nonmotor Symptoms

Object exploration test

In the center of the open box (W × D × H: 60 × 60 × 30 cm), a cylinder item (diameter, 5.5 cm; height, 13 cm) was exposed. A rat was placed in the open box with its back to the test object and given 10 minutes to explore. The time it took for a rat to approach an object and the duration of each subsequent approach were recorded.

Light/dark box test

Rats were examined in 2 compartments (W × D × H: 60 × 30 × 30 cm), which were connected together length-wise. There was a 10 × 10 cm square aperture between the 2 compartments that the rat could utilize and move between. One chamber was

closed with a lid (i.e., the dark box), whereas the other was white, left uncovered, and illuminated with an 880-lux light (i.e., the light box). Again, the rat was allowed 10 minutes to explore both chambers. Here, both the frequency of entry and the duration spent in the light box were calculated.

Forced swim test

This test exposed the rats to a cylindrical container (diameter, 20 cm; height, 70 cm) containing water at a temperature of 24°C ± 1°C and a depth of 30 cm. The duration of time the rat floated upright without moving or 'struggling' — aside from efforts to maintain its head above water — was known as the time spent in immobility.

Immunohistochemistry

All immunohistochemistry methods were followed as described in previous studies [22,23]. The fixed brain hemispheres were sectioned in the coronal plane to a 30-µm thickness. To inactivate endogenous peroxidase activity, free-floating sections were incubated in 0.3% (v/v) hydrogen peroxide for 20 minutes before being blocked with 5% (v/v) normal goat serum (Vector ABC Elite Kit; Vector Laboratories, Burlingame, CA, USA) in 0.3% (v/v) Triton X-100 for 1 hour at room temperature (RT; 22°C ± 2°C). Sections were then incubated overnight at 4°C with rabbit anti-tyrosine hydroxylase (TH; 1:500; Millipore, Darmstadt, Germany), rabbit anti-glial fibrillary acidic protein (GFAP; 1:2,000; Dako, Glostrup, Denmark), or the rabbit anti-ionized calcium-binding adapter molecule 1 (Iba1; 1:1,000; Wako, Osaka, Japan). Sections were incubated for 1 hour at RT with biotinylated goat anti-rabbit IgG (Vector ABC Elite Kit), and then incubated for 1 hour at RT with an avidin-biotin-peroxidase complex (Vector ABC Elite Kit). The peroxidase reaction was induced using a diaminobenzidine substrate (DAB kit; Vector Laboratories).

Three hemisections of the SN (approximately 5.08 mm caudally from the bregma) were selected from each rat for cell counting. The mean number of immunopositive cells in the 3 sections of each rat was taken as n = 1. Moreover, the images were converted to grayscale to measure TH immunoreactivity in the striatum (approximately 0.26 mm caudally from the bregma) alongside GFAP and Iba1 immunoreactivities in the hippocampus (approximately 3.80 mm caudally from the bregma). The mean gray value (256 gray levels) was calculated using ImageJ software (NIH, Bethesda, MD, USA) for each chosen area. The relative changes in intensity levels of TH+, GFAP+,

and Iba1+ immunoreactivities were expressed as relative to their optical densities (ODs) after setting the mean intensity of the control to 1. The number and intensity of the immunopositive cells per group were averaged and expressed as mean \pm standard error (SE; n = 3 rats/group).

Western Blotting

All Western blot protocols were followed as described in previous studies [22,23]. Electrophoresis was used to separate proteins on 7%–15% sodium dodecyl sulfate polyacrylamide gel. The proteins were subsequently transferred to polyvinylidene difluoride membranes. The membranes were then blocked for 1 hour at RT with 1% (v/v) bovine serum albumin (Sigma-Aldrich) and 2% (v/v) NGS (Vector Laboratories) in phosphate-buffered saline (PBS) containing 0.1% (v/v) Tween 20 (PBS-T; pH 7.4). The membranes were subsequently treated overnight at 4°C with rabbit anti-GFAP (1:2,000) and Iba1 (1:1,000) pri-

mary antibodies. The membranes were incubated with horseradish peroxidase-conjugated goat anti-rabbit IgG antibody (Vector Laboratories) for 1 hour at RT, and the signals were detected using a chemiluminescence kit (SuperSignal West Pico; Thermo Fisher Scientific, Waltham, MA, USA). After stripping, the membranes were probed again with the mouse anti- β -actin antibody (1:5,000; Sigma-Aldrich) for 2 hours at RT. The OD of each band was assessed using an iBright CL750 Imaging System (Thermo Fisher Scientific).

Golgi Staining

The dendritic complexity, spine density, and spine morphology of the neurons in the hippocampal CA1 and DG subregions were studied using Golgi impregnation. The FD Rapid Golgistain Kit and accompanying techniques were employed in accordance with the manufacturer's guidelines (FD Neurotechnologies, Ellicott City, MD, USA).

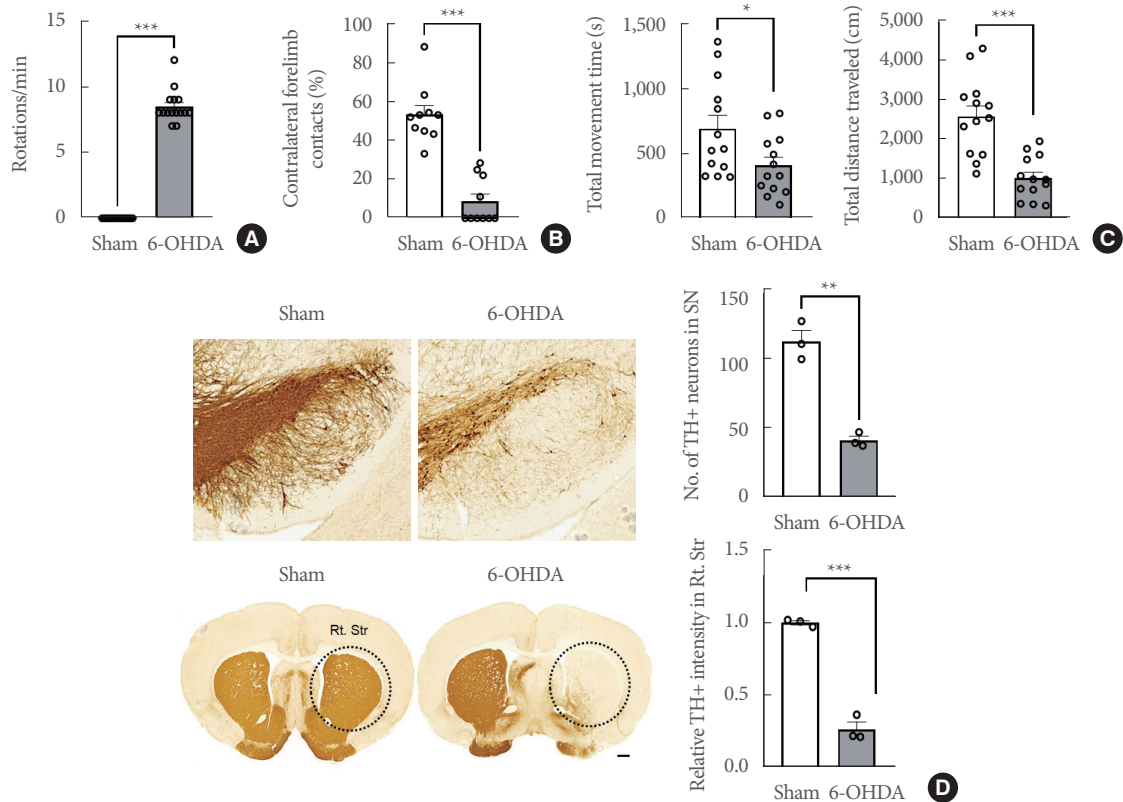


Fig. 1. Impairments of motor functions and nigrostriatal DAergic signaling in the unilateral 6-OHDA-lesioned hemiparkinsonian rat model. (A) Apomorphine rotation test (n = 15 rats/group). (B) Cylinder test (n = 10 rats/group). (C) Open field test (n = 13 rats/group). (D) Representative photomicrographs and bar graphs (n = 3 rats/group) showing immunoreactivities of TH+ cells in the SN (upper panels, scale bar = 100 μ m) and TH+ fibers in the striatum (lower panels, scale bar = 1,000 μ m). Data are expressed as the mean \pm standard error. 6-OHDA, 6-hydroxydopamine-lesioned group; Rt. Str, right striatum; Sham, sham-operated controls; SN, substantia nigra; TH, tyrosine hydroxylase. *P < 0.05. **P < 0.01. ***P < 0.001.

Sholl Analysis

As previously reported [22,23], both CA1 and DG neurons of the hippocampus were traced and analyzed. Using a camera lucida at a magnification of 200×, 10 neurons from each hippocampal region were randomly dispersed among 3 brain slices (approximately 3.80 mm behind bregma) in each animal. Sholl's concentric circle method [22,23] was used to objectively examine the dendrites for each of the chosen neurons. Dendrites intersecting each circle were counted to determine the number of dendritic intersections at different radial distances from the neuronal soma, in addition to the total dendritic length, and branch points. Each value was averaged per rat, and the mean value of each rat was taken as n=1. The value per group was averaged and expressed as mean ± SE (n=8 rats/group).

Measurement of Spine Density and Morphology

All discernible projecting dendritic spines were counted along 30-µm dendritic segments from the terminal to the tip of 3 dendrites from each neuron using 1,500× magnification. Spines were divided into the following morphological categories: (1) thin: spines with a discernible small head and an extended neck, (2) mushroom: spines with a voluminous head and a noticeable neck, and (3) stubby: spines with an overall stubby look and no discernible neck. Ten segments were counted in each animal

(n=8 rats/group), and the spine density was determined as the number of spines per 10 µm of dendritic length.

Statistical Analysis

All statistical analyses were performed using Prism (GraphPad Software, San Diego, CA, USA; RRID: SCR_002798). The changes between the number of dendritic intersections at different radial distances of the sham-operated controls and 6-OHDA-lesioned rats were identified, for 8 rats per group, using two-way repeated-measures analysis of variance followed by multiple comparison tests corrected with Šidák's *post hoc* test. Unpaired Student t-tests were used for all other analyses to compare the means of the sham-operated controls and 6-OHDA-lesioned rats. For all statistical tests, a P-value <0.05 was considered statistically significant.

RESULTS

Striatal 6-OHDA Infusion Induced Motor dysfunctions and Deceased TH+ Immunoreactivity in the Nigrostriatal Pathway

Initially, motor impairments and nigrostriatal DAergic degradation in the study's hemiparkinsonian rat model were confirmed. At 4 weeks postsurgery, rats having >7 rotations/min

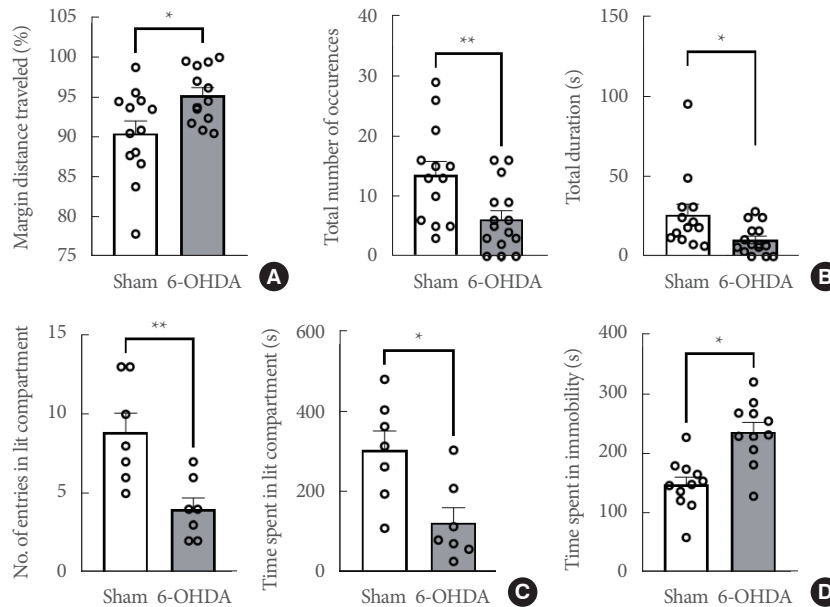


Fig. 2. Depression and anxiety-like nonmotor symptoms in the unilateral 6-OHDA-lesioned hemiparkinsonian rat model. (A) Margin distance traveled (%) in the open field test (n=13 rats/group). (B) Object exploration test (n=13 rats/group). (C) Light/dark box test (n=7 rats/group). (D) Forced swim test (n=11 rats/group). Data are expressed as the mean ± standard error. 6-OHDA, 6-hydroxydopamine-lesioned group; Sham, sham-operated controls. *P < 0.05. **P < 0.01.

due to apomorphine treatment (n = 15 rats/group) were regarded as effectively induced hemiparkinsonian models (t(28) = 26.32; P < 0.0001) (Fig. 1A). At 6 weeks postsurgery, the cylinder test (n = 10 rats/group) showed that right-side hemiparkinsonian rats exhibited a significantly reduced use of the left forelimb, resulting in an ~60% decrease in the left/right ratio of forelimb usage (t(18) = 7.431, P < 0.0001) (Fig. 1B). Locomotor activity in the open field (n = 13 rats/group) revealed that rats with unilaterally striatal 6-OHDA infusion display a significantly lower total distance traveled (t(24) = 5.014, P < 0.05) and total movement time (t(24) = 2.340, P < 0.0001) than the sham-

operated controls (Fig. 1C). Additionally, the TH+ immunoreactivity in the *substantia nigra* and striatum were examined to validate the suppression of the ipsilateral DAergic signal pathway caused by unilateral 6-OHDA infusion (Fig. 1D). The lesion extent measurement using TH+ cell immunoreactivity revealed significant deterioration in the ipsilateral *substantia nigra* (t(4) = 8.409, P < 0.01) and striatum (t(4) = 14.11, P < 0.0001).

Striatal 6-OHDA Infusion Induced Anxiety and Depression-Like Behaviors in Rats

Since anxiety and depression are significant nonmotor features

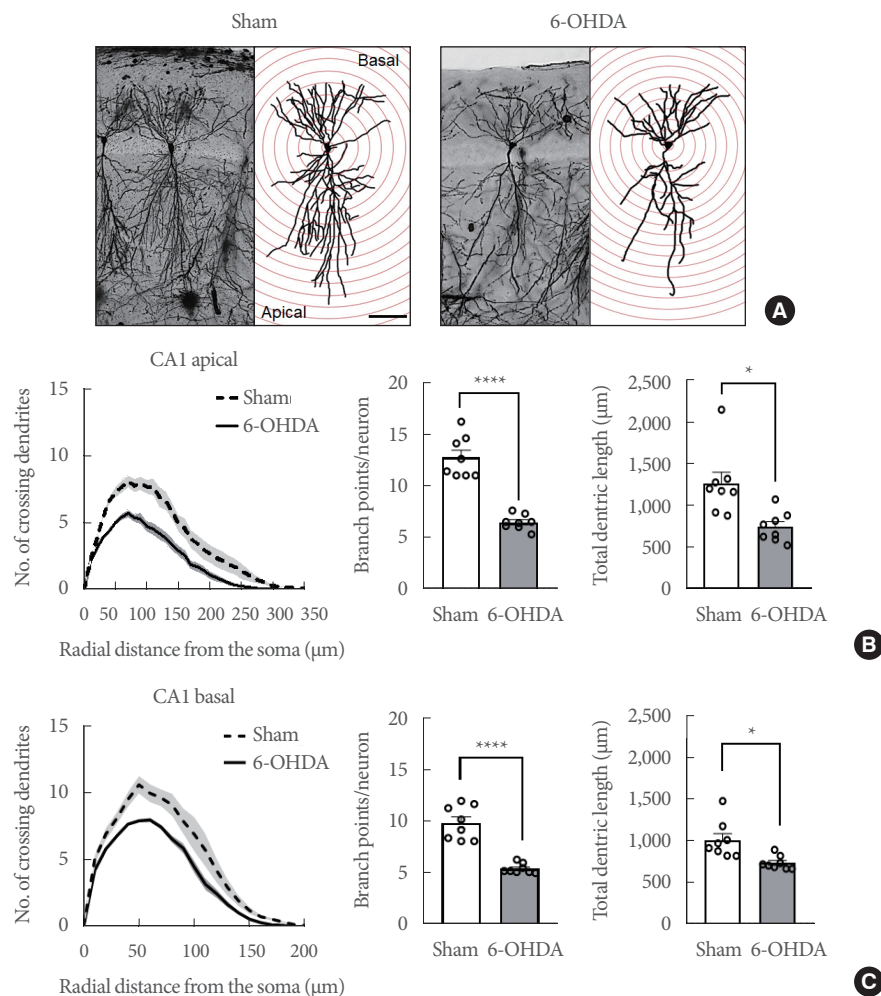


Fig. 3. Striatal 6-OHDA infusion affects the dendritic complexity of the ipsilateral conus ammonis 1 (CA1) pyramidal neurons in rats. (A) Representative Golgi-stained images of the CA1 subregion in sham-operated controls and 6-OHDA-lesioned rats at a lower magnification (Scale bars = 50 µm). (B) Line and bar graphs showing the mean number of intersections (left panel), dendritic branch point count (middle panel), and the total dendritic length (right panel) in the CA1 apical dendrite. (C) Line and bar graphs showing the mean number of intersections (left panel), dendritic branch point count (middle panel), and the total dendritic length (right panel) in the CA1 basal dendrite. Data are expressed as the mean ± standard error (n = 8 rats/group). 6-OHDA, 6-hydroxydopamine-lesioned group; Sham, sham-operated controls. *P < 0.05. ****P < 0.0001.

of PD [8], anxiety- and depression-like behaviors were assessed in hemiparkinsonian rats. We employed several paradigms for those behaviors, including the open field test, object exploration, light/dark box test, and the forced swim test (Fig. 2). In the open field test (n = 13 rats/group), the margin in distance traveled and total distance traveled (%) was significantly increased in 6-OHDA-lesioned rats ($t(24) = 2.622, P < 0.05$) (Fig. 2A). Additionally, the total number of occurrences (approaching frequency) in 6-OHDA-lesioned rats was significantly lower than in sham-operated controls ($t(26) = 2.862, P < 0.01$) in the object exploration test (n = 13 rats/group, Fig. 2B). The total duration time (approaching time) was significantly shorter in the 6-OHDA-lesioned rats than in the sham-operated controls ($t(26) = 2.362, P < 0.05$). The 6-OHDA-lesioned rats had fewer entries into the illuminated compartment ($t(12) = 3.417, P < 0.01$) and spent less time in the light box compartment ($t(12) = 2.983, P < 0.05$) in the light/dark box test (n = 7 rats/group, Fig. 2C). Finally, the 6-OHDA-lesioned rats displayed a longer immobility time (considered an index of depression) compared to sham-operated controls ($t(20) = 4.352, P < 0.001$)

in the forced swim test (n = 11 rats/group, Fig. 2D).

6-OHDA-Lesioned Rats Displayed Significant Reduction in Dendritic Arborization of Hippocampal Neurons in the CA1 and DG Subregions

Eight weeks following the striatal 6-OHDA infusion, Golgi staining was used to track and quantify the dendritic complexity of the ipsilateral CA1 and DG neurons. The number of dendritic intersections was counted at various radial distances from the neuronal soma using Sholl analysis (Figs. 3A, 4A, n = 8 rats/group). At Sholl radii of 30–170 μm from the soma, the CA1 apical dendrites in the hippocampi of 6-OHDA-lesioned rats had significantly fewer intersections than those in sham-operated controls (Fig. 3B, left panel; $F_{interaction} [34, 2652] = 10.44, P < 0.0001$). The number of branching points in the CA1 apical dendrites in 6-OHDA-lesioned rats was significantly lower than in sham-operated controls (Fig. 3B, middle panel; $t(14) = 8.317, P < 0.0001$). Moreover, striatal 6-OHDA infusion significantly reduced the total length of the CA1 apical dendrite in the hippocampi of rats (Fig. 3B, right panel: $t(14) = 3.394, P < 0.01$). In

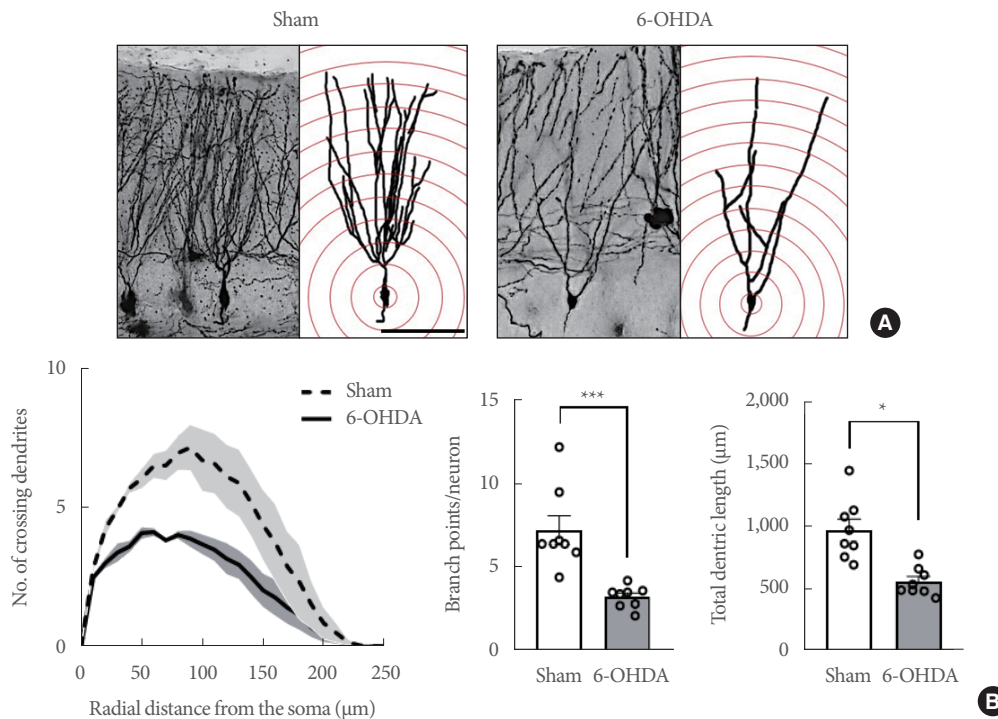


Fig. 4. Striatal 6-OHDA infusion affects the dendritic complexity of the ipsilateral dentate gyrus (DG) granular neurons in rats. (A) Representative Golgi-stained images of the DG subregion in sham-operated controls and 6-OHDA-lesioned rats at a lower magnification (Scale bars = 50 μm). (B) Line and bar graphs showing the mean number of intersections (left panel), dendritic branch point count (middle panel), and the total dendritic length (right panel) in the DG neurons. Data are expressed as the mean ± standard error (n = 8 rats/group). 6-OHDA, 6-hydroxydopamine-lesioned group; Sham, sham-operated controls. *P < 0.05. ***P < 0.001.

the hippocampal CA1 basal, the dendrites in 6-OHDA-lesioned rats had fewer intersections than those in sham-operated controls at Sholl radii of 20–110 μm from the soma (Fig. 3C, left panel; $F_{\text{interaction}} [20, 1,560] = 9.049, P < 0.0001$). Striatal 6-OHDA infusion significantly decreased both the number of branch points (Fig. 3C, middle panel; $t(14) = 7.353, P < 0.0001$) and the total length (Fig. 3C, right panel; $t(14) = 3.265, P < 0.01$) of the CA1 basal dendrites in rat hippocampi.

Further, the neuronal dendrites in the hippocampal DG of 6-OHDA-lesioned rats exhibited fewer intersections than the sham-operated controls at Sholl radii of 20–150 μm from the soma (Fig. 4B, left panel; $F_{\text{interaction}} [24, 1,872] = 10.45, P < 0.0001$). The dendritic branch points (Fig. 4B, middle panel; $t(14) = 4.458, P < 0.001$) and total dendritic length (Fig. 4B, right panel; $t(14) = 4.344, P < 0.001$) of DG neurons were significantly different between the sham-operated controls and 6-OHDA-lesioned rats.

Striatal 6-OHDA Infusion Significantly Altered Dendritic Spine Density and Morphology in the Hippocampal CA1 and DG Subregions

The Golgi-stained neurons were magnified and their dendritic spine density and morphology were analyzed for any alterations (Fig. 5A–C, left panels). The dendritic spine densities (the number of spines per 10- μm dendrite) were significantly decreased in the apical CA1 (Fig. 5A, middle panel; $t(14) = 3.158, P < 0.01$), basal CA1 (Fig. 5B, middle panel; $t(14) = 3.397, P < 0.01$), and DG (Fig. 5C, middle panel; $t(14) = 2.183, P < 0.05$) of the 6-OHDA-lesioned rats.

Moreover, variations in the proportion of dendritic morphology were found in the subregions of the hippocampus. The proportion of thin spines (% in 10- μm dendrite) was significantly increased in the CA1 apical (Fig. 5A, right panel; $t(14) = 3.8, P < 0.01$) and DG subregions (Fig. 5C, right panel; $t(14) = 4.9, P < 0.001$) in 6-OHDA-lesioned rats. Conversely, the pro-

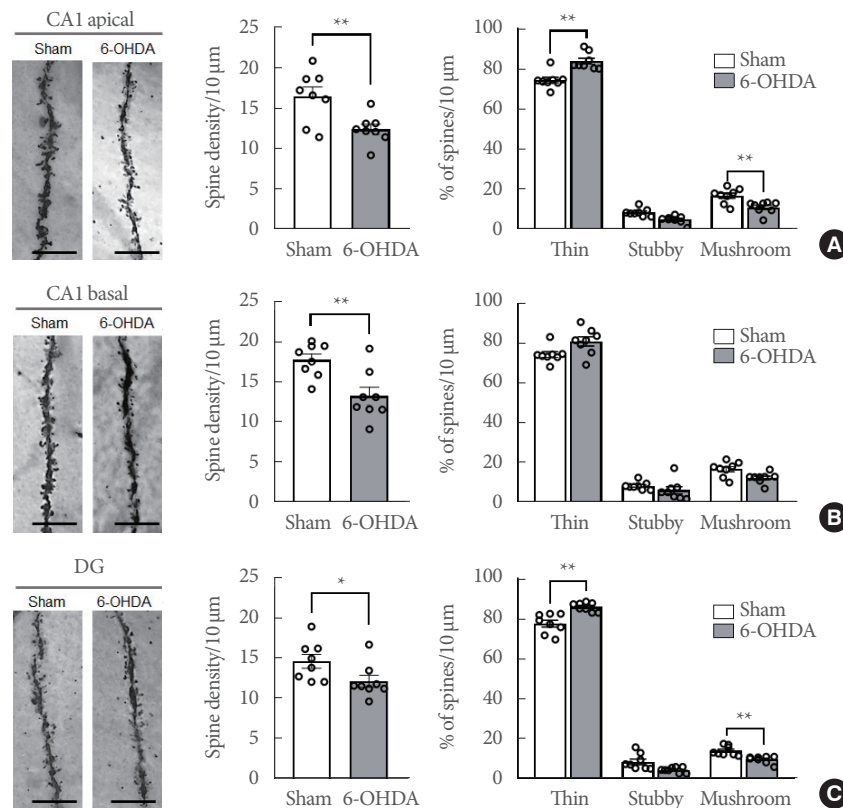


Fig. 5. Striatal-6-OHDA infusion alters the dendritic spine density and morphology in the ipsilateral hippocampal conus ammonis 1 (CA1) and dentate gyrus (DG) of rats. (A) CA1 apical dendrites. (B) CA1 basal dendrites. (C) DG dendrites. Representative photos (Scale bars = 5 μm) show dendritic spines in each subregion (A–C, left panels). Bar graphs display the spine density per 10 μm of the dendrite (A–C, middle panels) and spine morphology per 10 μm of the dendrite (A–C, right panels) in each subregion. Data are expressed as the mean \pm standard error ($n = 8$ rats/group). 6-OHDA, 6-hydroxydopamine-lesioned group; Sham, sham-operated controls. * $P < 0.05$. ** $P < 0.01$.

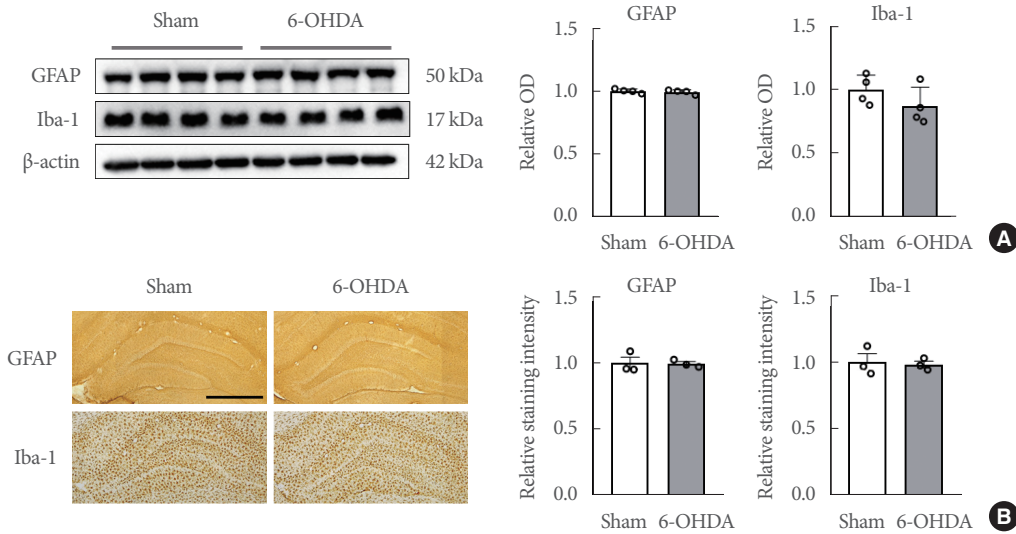


Fig. 6. Striatal 6-OHDA infusion does not affect the astrocytic and microglial activity and distribution in the ipsilateral hippocampus of rats. (A) Immunoblots of GFAP (a marker for astrocytes) and Iba1 (a marker for microglia) (n=4 rats/group). (B) Representative photos (upper panels, scale bars = 100 μm) and bar graphs (lower panels) showing the levels of Iba-1 and GFAP immunoreactivities in the hippocampus in each group (n=3 rats/group). Data are expressed as means ± standard error. 6-OHDA, 6-hydroxydopamine-lesioned group; Sham, sham-operated controls; GFAP, glial fibrillary acidic protein; Iba1, ionized calcium-binding adapter molecule 1; OD, optical density.

portion of mushroom spines was significantly decreased in the CA1 apical (Fig. 5A, right panel; $t(14)=2.7, P<0.05$) and DG subregions (Fig. 5C, right panel; $t(14)=5.3, P<0.001$) in 6-OHDA-lesioned rats. However, there is no significant difference in the proportion of the CA1 basal dendrites spine morphology between sham-operated controls and 6-OHDA-lesioned rats (Fig. 5B, right panel).

Striatal 6-OHDA Infusion Did Not Activate Microglia and Astrocytes in the Ipsilateral Hippocampi

Western blot analysis illustrated no significant differences in protein levels of GFAP ($t(6)=0.5705, P=0.5890$) and Iba-1 ($t(6)=0.4892, P=0.6421$) in the hippocampi (Fig. 6A). Immunohistochemistry revealed that the expression intensities of GFAP ($t(4)=0.0879, P=0.9342$) and Iba-1 ($t(4)=0.2757, P=0.7964$) in the hippocampus were unaffected by striatal 6-OHDA infusion (Fig. 6B).

DISCUSSION

In this study, unilaterally striatal 6-OHDA infusion produced persistent motor (hypolocomotion and asymmetric behavioral deficit) and nonmotor (anxiety/depression-like behaviors) symptoms. Additionally, it induced the destruction of DAergic

signaling in the ipsilateral nigrostriatal pathway of rats; identified through the loss of TH+ neurons in the SN and TH+ fibers in the striatum. Intriguingly, the striatal 6-OHDA infusion significantly altered neuronal architecture (dendritic complexity alongside spine density and morphology) in the ipsilateral hippocampus and independently of neuroinflammation.

Pathological characteristics of PD include nigrostriatal DAergic degradation, which affects motor function [24]. Asymmetries in sensorimotor reactivity beginning 6 weeks [25] and impairments in motor coordination and balance abilities at 2 weeks [26] are the most noticeable deficiencies observed in unilateral 6-OHDA-infused rats. Indeed, in this study, rats with striatal 6-OHDA infusion were subjected to a complete evaluation of PD-like behaviors utilizing multiple behavioral paradigms for assessing motor and nonmotor symptoms. Similar to previous studies [27], the present study uncovered noteworthy anxiety- and depression-like behaviors in rats infused unilaterally with 6-OHDA. Therefore, we found that striatal 6-OHDA infusion generated both motor and nonmotor dysfunctions, including anxiety/depression-like behaviors, which are associated with hippocampal dysfunctions.

DA affects hippocampal LTP [9] along with hippocampus-dependent learning and memory [28]. The hippocampus is implicated in the nonmotor dysfunctions of PD [8], and hippo-

campal neuroplasticity interacts with the DAergic system in PD [10]. Here, we focused on the modification of structural plasticity in the hippocampus of PD. In this study, striatal 6-OHDA infusion significantly decreased the dendritic complexity and spine density in the ipsilateral hippocampus, suggesting that the destruction of DAergic signaling downregulates structural plasticity in a hippocampus with PD. Additionally, striatal 6-OHDA infusion altered the morphology of spines on hippocampal dendrites (thin spines increased and mushroom spines decreased), which suggests that impaired spine maturation may lead to a decrease in postsynaptic density and excitatory neurotransmission [29]. There are several possible mechanisms underlying the alteration of structural plasticity in the hippocampus after striatal 6-OHDA infusion. Mesencephalic DAergic neurons project to the limbic system, including the hippocampus, whilst it is known that DA receptors regulate cognition-related and synaptic plasticity-related processes in the hippocampus [30]. Indeed, Janakiraman et al. [31] discovered a decrease in DA and serotonin levels in the hippocampus following a chronic MPTP regimen. Furthermore, DA promotes dendritic growth, and DAergic deficiency leads to shorter dendrites and a lower spine density in the nucleus accumbens [32]. Thus, this study suggests that prolonged DA depletion may alter structural plasticity in the hippocampus. These findings might point to interactions between DAergic transmission and hippocampal neuroplasticity for nonmotor symptoms in PD.

According to a previous study, neuroinflammation is potentially one of the key causes that leads to synaptic and cognitive impairments in neurodegenerative diseases [33]. Microglia and astrocytes are activated in various neurodegenerative diseases, including PD, Alzheimer disease, and multiple sclerosis [34]. Activated microglia and astrocytes may play potentially detrimental roles by eliciting the expression of proinflammatory cytokines [35]. However, neither microglial nor astrocytic activation was found in the hippocampus following striatal 6-OHDA infusion in this study. Ultimately, this indicates that neuroinflammation does not necessarily promote the decrease of structural plasticity and hippocampal dysfunction. Furthermore, RNA-sequencing demonstrated no significant alterations in neuroinflammation-related genes in the hippocampus between sham-operated controls and 6-OHDA-lesioned rats (data not shown).

Overall, rats with striatal 6-OHDA infusion displayed motor and nonmotor symptoms as well as nigrostriatal DA degeneration. In addition, striatal 6-OHDA infusion affected dendritic

complexity along with spine density, and morphology in the ipsilateral hippocampus of rats. These findings demonstrate that in a PD animal model, inhibiting the DAergic pathway causes changes to the neuronal architecture in the hippocampus, independently of neuroinflammation. Consequently, this study provides anatomical evidence that structural plasticity in the hippocampus may play a role in the etiology of the nonmotor hallmarks of PD. Nonetheless, further research is required to establish the alterations in other neuroplasticity-related signals in the hippocampus in PD.

AUTHOR CONTRIBUTION STATEMENT

- Conceptualization: *CM*
- Data curation: *BK, CM*
- Formal analysis: *BK, PDEWM, MJA, JL, SK, CM*
- Funding acquisition: *CM*
- Methodology: *BK, PDEWM, MJA, JL, SK, JCK, SHK, JSK, CJ, TS, CM*
- Project administration: *CM*
- Visualization: *BK, PDEWM, MJA, JL, CM*
- Writing - original draft: *BK, CM*
- Writing - review & editing: *BK, CM*

ORCID

Bohye Kim	0000-0002-0970-1079
Poornima D. E. Weerasinghe-Mudiyanse	0000-0002-3753-0844
Mary Jasmin Ang	0000-0003-0998-3069
Jeongmin Lee	0000-0002-4535-2312
Sohi Kang	0000-0003-4689-5797
Jong-Choon Kim	0000-0002-8265-9911
Sung-Ho Kim	0000-0002-1884-6237
Joong-Sun Kim	0000-0003-2180-4860
Chaeyong Jung	0000-0002-5557-4576
Taekyun Shin	0000-0002-9851-4354
Changjong Moon	0000-0003-2451-0374

REFERENCES

1. GBD 2016 Dementia Collaborators. Global, regional, and national burden of Alzheimer's disease and other dementias, 1990-2016: a systematic analysis for the Global Burden of Disease Study 2016. *Lancet Neurol* 2019;18:88-106.

2. Van Den Eeden SK, Tanner CM, Bernstein AL, Fross RD, Leim-peter A, et al. Incidence of Parkinson's disease: variation by age, gender, and race/ethnicity. *Am J Epidemiol* 2003;157:1015-22.
3. Weerasinghe-Mudiyanselage PDE, Kang S, Kim JS, Moon C. Thera-peutic approaches to nonmotor symptoms of parkinson's disease: a current update on preclinical evidence. *Curr Neuropharmacol* 2022 Oct 5. <https://www.doi.org/10.2174/1570159X20666221005090126>. [Epub].
4. Maetzler W, Berg D. Parkinson disease in 2017: changing views af-ter 200 years of Parkinson disease. *Nat Rev Neurol* 2018;14:70-2.
5. Bang Y, Lim J, Choi HJ. Recent advances in the pathology of pro-dromal nonmotor symptoms olfactory deficit and depression in Parkinson's disease: clues to early diagnosis and effective treatment. *Arch Pharm Res* 2021;44:588-604.
6. Barone P, Erro R, Picillo M. Quality of life and nonmotor symp-toms in Parkinson's disease. *Int Rev Neurobiol* 2017;133:499-516.
7. Brandao PRP, Munhoz RP, Grippe TC, Cardoso FEC, de Almeida ECBM, Titze-de-Almeida R, et al. Cognitive impairment in Par-kinson's disease: a clinical and pathophysiological overview. *J Neurol Sci* 2020;419:117177.
8. Weerasinghe-Mudiyanselage PDE, Ang MJ, Kang S, Kim JS, Moon C. Structural plasticity of the hippocampus in neurodegenerative diseases. *Int J Mol Sci* 2022;23:3349.
9. Bliss TV, Collingridge GL, Morris RG, Reymann KG. Long-term potentiation in the hippocampus: discovery, mechanisms and function. *Neuroforum* 2018;24:A103-20.
10. Calabresi P, Castrioto A, Di Filippo M, Picconi B. New experimen-tal and clinical links between the hippocampus and the dopami-nergic system in Parkinson's disease. *Lancet Neurol* 2013;12:811-21.
11. Esmaeili-Mahani S, Haghparast E, Nezhadi A, Abbasnejad M, Sheibani V. Apelin-13 prevents hippocampal synaptic plasticity im-pairment in Parkinsonism rats. *J Chem Neuroanat* 2021;111: 101884.
12. Costa C, Sgobio C, Siliquini S, Tozzi A, Tantucci M, Ghiglieri V, et al. Mechanisms underlying the impairment of hippocampal long-term potentiation and memory in experimental Parkinson's dis-ease. *Brain* 2012;135:1884-99.
13. Schaefer AT, Teuchert-Noodt G. Developmental neuroplasticity and the origin of neurodegenerative diseases. *World J Biol Psychia-try* 2016;17:587-99.
14. Keller TA, Just MA. Structural and functional neuroplasticity in human learning of spatial routes. *Neuroimage* 2016;125:256-66.
15. Hotulainen P, Hoogenraad CC. Actin in dendritic spines: connect-ing dynamics to function. *J Cell Biol* 2010;189:619-29.
16. Verkhatsky A, Rodriguez JJ, Parpura V. Astroglia in neurological diseases. *Future Neurol* 2013;8:149-58.
17. Wang Y, Feng L, Liu S, Zhou X, Yin T, Liu Z, et al. Transcranial magneto-acoustic stimulation improves neuroplasticity in hippo-campus of Parkinson's disease model mice. *Neurotherapeutics* 2019;16:1210-24.
18. Weerasinghe-Mudiyanselage PDE, Ang MJ, Wada M, Kim SH, Shin T, Yang M, et al. Acute MPTP treatment impairs dendritic spine density in the mouse hippocampus. *Brain Sci* 2021;11:833.
19. Sepulveda B, Mesias R, Li X, Yue Z, Benson DL. Short- and long-term effects of LRRK2 on axon and dendrite growth. *PLoS One* 2013;8:e61986.
20. Winner B, Melrose HL, Zhao C, Hinkle KM, Yue M, Kent C, et al. Adult neurogenesis and neurite outgrowth are impaired in LRRK2 G2019S mice. *Neurobiol Dis* 2011;41:706-16.
21. Schultz W. Depletion of dopamine in the striatum as an experi-mental model of parkinsonism: direct effects and adaptive mecha-nisms. *Prog Neurobiol* 1982;18:121-66.
22. Ang MJ, Kang S, Moon C. Melatonin alters neuronal architecture and increases cysteine-rich protein 1 signaling in the male mouse hippocampus. *J Neurosci Res* 2020;98:2333-48.
23. Kang S, Lee S, Kim J, Kim JC, Kim SH, Son Y, et al. Chronic treat-ment with combined chemotherapeutic agents affects hippocampal micromorphometry and function in mice, Independently of neu-roinflammation. *Exp Neurobiol* 2018;27:419-36.
24. Guatteo E, Berretta N, Monda V, Ledonne A, Mercuri NB. Patho-physiological features of nigral dopaminergic neurons in animal models of Parkinson's disease. *Int J Mol Sci* 2022;23:4508.
25. Grealish S, Mattsson B, Draxler P, Bjorklund A. Characterisation of behavioural and neurodegenerative changes induced by intranigral 6-hydroxydopamine lesions in a mouse model of Parkinson's dis-ease. *Eur J Neurosci* 2010;31:2266-78.
26. Su RJ, Zhen JL, Wang W, Zhang JL, Zheng Y, Wang XM. Time-course behavioral features are correlated with Parkinson's disease-associated pathology in a 6-hydroxydopamine hemiparkinsonian rat model. *Mol Med Rep* 2018;17:3356-63.
27. Antunes MS, Cattelan Souza L, Ladd FVL, Ladd A, Moreira AL, Bortolotto VC, et al. Hesperidin ameliorates anxiety-depressive-like behavior in 6-OHDA model of Parkinson's disease by regulat-ing striatal cytokine and neurotrophic factors levels and dopami-nergic innervation loss in the striatum of mice. *Mol Neurobiol* 2020;57:3027-41.
28. Borgkvist A, Malmlof T, Feltmann K, Lindskog M, Schilstrom B. Dopamine in the hippocampus is cleared by the norepinephrine transporter. *Int J Neuropsychopharmacol* 2012;15:531-40.

29. Koyama Y, Hattori T, Nishida T, Hori O, Tohyama M. Alterations in dendrite and spine morphology of cortical pyramidal neurons in DISC1-binding zinc finger protein (DBZ) knockout mice. *Front Neuroanat* 2015;9:52.
30. Yoon DH, Yoon S, Kim D, Kim H, Baik JH. Regulation of dopamine D2 receptor-mediated extracellular signal-regulated kinase signaling and spine formation by GABAA receptors in hippocampal neurons. *Neurosci Lett* 2015;586:24-30.
31. Janakiraman U, Manivasagam T, Thenmozhi AJ, Essa MM, Barathidasan R, SaravanaBabu C, et al. Influences of Chronic Mild Stress Exposure on Motor, Nonmotor Impairments and Neurochemical Variables in Specific Brain Areas of MPTP/Probenecid Induced Neurotoxicity in Mice. *PLoS One* 2016;11:e0146671.
32. Meredith GE, Ypma P, Zahm DS. Effects of dopamine depletion on the morphology of medium spiny neurons in the shell and core of the rat nucleus accumbens. *J Neurosci* 1995;15:3808-20.
33. Sy HN, Wu SL, Wang WF, Chen CH, Huang YT, Liou YM, et al. MPTP-induced dopaminergic degeneration and deficits in object recognition in rats are accompanied by neuroinflammation in the hippocampus. *Pharmacol Biochem Behav* 2010;95:158-65.
34. Thameem Dheen S, Kaur C, Ling EA. Microglial activation and its implications in the brain diseases. *Curr Med Chem* 2007;14:1189-97.
35. Cheung YT, Lim SR, Ho HK, Chan A. Cytokines as mediators of chemotherapy-associated cognitive changes: current evidence, limitations and directions for future research. *Plos One* 2013;8:e81234.